FUDMA Journal of Engineering and Technology
ISSN: 3092-9385
https://sites.google.com/fudutsinma.edu.ng/fjet
Volume 1, Issue 2, 2025, 819-832

Performance Evaluation of Fuzzy Logic and Fractional Order PI Controllers for Electric Vehicle Wireless Charging System

Aminu BALA[1*], Nasiru B. KADANDANI[2,3], Isiyaku ABUBAKAR[4]

[1*]Department of Electrical and Electronics Engineering, Federal University Dutsin-Ma, Katsina State, Nigeria
[2]Department of Electrical and Electronics Engineering, Federal University of Transportation, Daura, Katsina State, Nigeria
[3,4]Department of Electrical Engineering, Bayero University, Kano, Nigeria

[1*]abbal@fudutsinma.edu.ng, [2,3]nbkadandani.ele@buk.edu.ng, [4]iabubakar.ele@buk.edu.ng

Abstract

This study presents a comprehensive performance evaluation of fuzzy logic controller (FLC) and fractional order proportional integral (FOPI) controller applied to an electric vehicle (EV) wireless charging system. A comparative analysis was conducted through detailed simulation models in MATLAB software R2021a to assess the controllers' effectiveness in maintaining regulated and stable output voltage and power transfer efficiency. Although both FLC and FOPI controllers have been explored in various nonlinear systems, limited comparative performance studies exist on their application to EV wireless charging systems under identical simulation conditions. Moreover, most previous works focus on conventional PID control and do not compare intelligent controllers (like Fuzzy and FOPI). The FLC was implemented in MATLAB software using FLC tool box to address system nonlinearities through rule-based system, while Fractional-Order Modeling and Control (FOMCON) tool box in MATLAB Simulink was utilized to obtain optimal parameters for FOPI controller. The optimized parameters obtained when integral time square error (ITSE) was used as performance matrix are proportional gain, k_p = 3.2555, integral gain, k_i = 2.5062 and λ =0.93 which improve control precision. Simulation outcomes revealed that FLC controller demonstrated superior dynamic performance in terms of power transfer efficiency of 89% compared to FOPI and open loop of 72&and 21.8% respectively. It was established that FOPI controller enhanced system stability with minimal overshoot and settling time compared to FLC. These results indicate that advanced control methodologies, such as FLC and FOPI controllers can substantially improve the operational reliability and efficiency of EV wireless charging systems by promoting wider adoption of wireless charging technologies.

Keywords: *Electric vehicles, wireless power, fuzzy controller, fractional order PI controller, DC-DC converter.*

1.0 Introduction

Electric vehicles (EVs) have gained popularity because of their improved efficiency, low carbon emissions, and superior performance over conventional internal combustion engine (ICE) [1]. The growth of EVs on the road has increased exponentially. So, the desired energy availability and recharge infrastructure in multi-energy systems must be in place to support this mass adoption [2]. The proliferation of new energy generation and storage resources has led to an increase in the complexity of the electrical network nowadays. These sources supply varied voltages (DC and AC) and frequencies for their electrical energy production. It is inevitable that new technologies will be used to control and enhance the power system's reliability because distribution networks and EV chargers are non-linear in nature, an efficient controller is required [3]. In light of these complications, Power generation, energy storage, and loads in a grid or micro grid must be connected through intelligent energy management (IEM) [4]. It is anticipated that power quality problems such voltage imbalance, transformer failure, and harmonic distortion may surface as electric vehicles (EVs) become more prevalent in distribution networks [3]. Electric vehicle (EV) charging methodologies are broadly categorized into wired and wireless systems. Wired conductive charging is further classified into three levels: Level 1 (L-1), Level 2 (L-2), and Level 3 (L-3)[5]. In contrast, wireless charging technologies are primarily divided into Capacitive Power Transfer (CPT) and Inductive Power Transfer (IPT), with IPT being the preferred technique due to its efficiency and reliability compared to CPT. Additionally, wireless charging methods are subdivided into static and dynamic approaches [42].Traditional wired power transmission faces challenges such as wear, aging, electrical sparking, and safety issues in difficult terrains like mountains and sea beds [6], wireless Power Transfer (WPT) offers a safer and more convenient alternative by eliminating physical connectors, enhancing reliability, and reducing user intervention [7]. Due to these advantages, WPT has seen growing adoption in homes, transportation hubs, docks, and industrial [8]. Wireless charging is expected to enable smaller, lighter, and more cost-effective EV batteries, particularly through dynamic charging systems. Major automakers such as Hyundai, Nissan, and Tesla are investing in this technology, although only a few current models support it. Overall, these developments indicate strong future growth in the wireless EV charging market [9].

Received: 06/11/2025; Revised: 01/12/2025; Accepted: 04/12/2025; Published: 22/12/2025

Inductive Power Transfer (IPT) is a wireless charging method that operates on the principle of electromagnetic induction [6]. It primarily comprises two essential elements: a transmitter coil and a receiver coil. An alternating current (AC) flowing through the transmitter coil produces a time-varying magnetic field, which, based on Faraday's law of electromagnetic induction, induces an electromotive force (EMF) in the receiver coil. This induced EMF generates current, facilitating the wireless transmission of electrical energy. As illustrated in Fig. 1, the IPT system involves an inverter on the transmitter side that produces a high-frequency AC. This AC generates the magnetic field required for power transfer. On the receiver side, the alternating current induced in the coil is converted into direct current (DC) using a rectifier, which is then used to charge a load such as a battery [10].

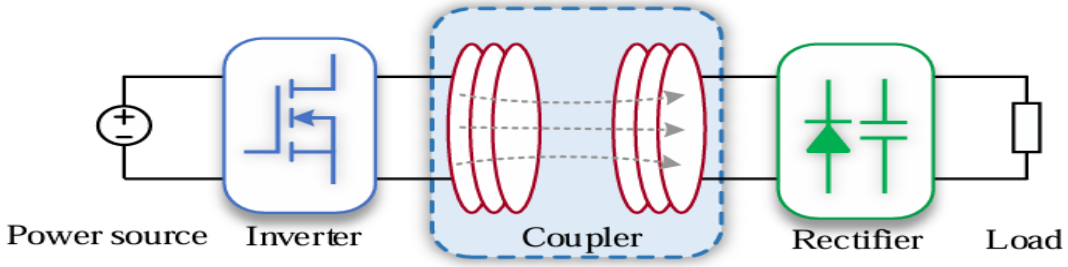

Figure 1: Principle of inductive power transfer (IPT) [10]

1.1 Literature Review

The global trend towards sustainable transportation has resulted in a significant increase in the number of electric vehicles (EVs). As EVs gain popularity, the desire for efficient and user-friendly charging options has become a vital part in promoting their widespread adoption [10][11].The review focuses on the fundamental principles of wireless power transfer, recent technological developments, system-level integration, and standardization efforts. It also examines the application of wireless charging in stationary and dynamic charging scenarios [12][10].

The research in[13] developed a nonlinear dynamic model for electric vehicles (EVs) by integrating both kinetic and electrical subsystems, with a primary focus on achieving robust speed control. To enhance system resilience and ensure effective disturbance rejection, various controllers were designed using multiple optimization techniques. The study in [14] employed metaheuristic algorithms to design a speed controller for a DC motor based on Fractional Order PID (FOPID) parameters. Computational intelligence techniques, including Particle Swarm Optimization (PSO) and Ant Colony Optimization (ACO), were utilized to efficiently tune controller parameters, yielding highly accurate results. System robustness was validated by introducing a disturbance signal with 0.1 noise power, where the FOPID controller demonstrated noise damping of approximately 30%, indicating improved stability. Comparative analysis confirmed that the FOPID controller significantly enhanced transient and time-domain responses, achieving minimal overshoot, rise time, settling time, and steady-state error. Literature in [15] proposed an efficient Adaptive Neuro-Fuzzy Inference System (ANFIS)-based Fractional Order PID (FOPID) controllers for electric vehicle (EV) speed tracking, where the vehicle is driven by a DC motor. The FOPID controller parameters were optimized using the Ant Colony Optimization (ACO) algorithm. The effectiveness of the ANFIS model was assessed using statistical performance metrics such as Mean Square Error (MSE), Root Mean Square Error (RMSE), and the coefficient of correlation (R). Performance metrics such as IAE, ITAE, ISE, and ITSE confirmed the effectiveness of the proposed controller, with the ANFIS-FOPID achieving notably low error values (MSE = 6.01×10^{-5}, MAE = 0.004, SSE = 2.65).

The whole EV wireless charging system was represented based on block diagram as shown in Fig.2.

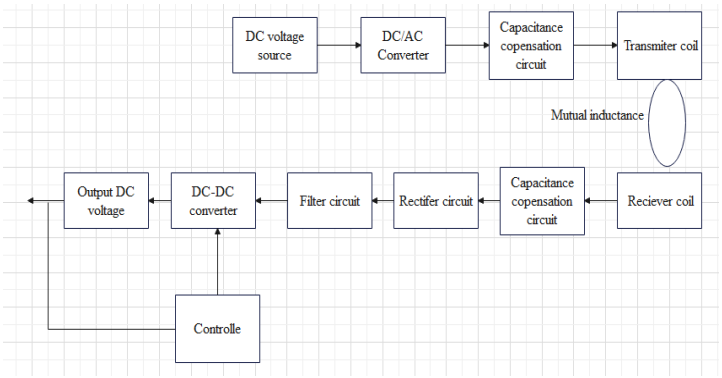

Figure 2: Block diagram of EV wireless charging system

Received: 06/11/2025; Revised: 01/12/2025; Accepted: 04/12/2025; Published: 22/12/2025

1.2 EV Wireless Charging Standard

The implementation of WPT systems is guided by various standards, with SAE J2954/1/2 defining essential parameters like alignment, interoperability, operating frequencies, power levels, and safety protocols, including obstacle detection, magnetic field limits, contact current, communication, temperature control, and electric shock protection e.tc. To standardize inductive charging for vehicle's batteries, the J2954 standard categorizes induction charging systems by nominal power and the distance from the secondary coil to the ground. This standard establishes four ranges and three classes. To avoid health risks related to magnetic radiation, the J2954 standard states that the public must not be exposed to magnetic fields exceeding $27\mu T$ at frequencies between 3 kHz and 10 MHz, as recommended by the International Commission on Non-Ionizing Radiation Protection. According to the SAE J2954 standard, charging stations are classified into four power levels, ranging from 3.7 kW to 22 kW. The station will provide an output of 22 kW with a battery voltage of 550V.According to the SAE J2954 standard, the designated resonant frequency for inductive charging systems is 85 kHz[9]. Consequently, this study will adopt a resonant frequency of $f_O = 85KHz$ for all analyses and calculations. Based on the electric vehicle market, the voltage range for the inductive charging station should be between 300 V and 550 V.

1.2 High Frequency Inverter for DC-AC Conversion

High frequency inverter was used to convert DC source voltage to AC. Utilizing high frequency in WPT allows for more efficient and precise energy transfer, potentially reducing interference and enabling smaller component sizes[11]. Higher frequencies are preferable when minimizing losses, reducing component size, and preventing local heating H-bridge topologies are often used in simulations as shown in Fig.3.

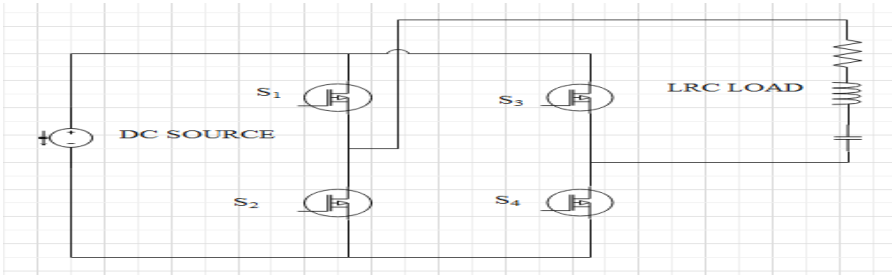

Figure 3: Higher frequency inverter diagram

The output voltage waveform of the DC-AC converter is square shaped. The converter's output voltage Fourier series is given as:

$$V_1(t) = \frac{4V_{in}}{\pi}\sum_{n=1}^{\infty}\frac{1-(-1)^n}{2n}\sin(n\omega t) \quad (1)$$

where $V_{in} = input\ voltage,\ n = an\ integer, and\ \omega = 2\pi f$

$$V_1(t) = \frac{4V_{in}}{\pi}\sin(n\omega t) \quad (2)$$

The H-bridge output voltage can now be represented as an AC voltage source, with the RMS value determined by the fundamental harmonic equation, as shown in equation (3).

$$V_P = \frac{2\sqrt{2}}{\pi}V_L \quad (3)$$

where $V_P = primary\ side\ voltage, V_L = load\ voltage$

1.4 Resonance Circuit Topology

To optimize power transfer, resonant compensation is employed to minimize inductance leakage and enhance coupling [39]. The principal compensation configurations for magnetic resonant WPT include the four primary compensation topologies, series-series (SS), series-parallel (SP), parallel-series (PS), and parallel-parallel (PP) which are frequently utilized for a variety of applications. The simplest compensation network topologies utilize a single capacitor, connected either in series (Fig.4) or in parallel (Fig.5), which resonates with the inductance of the corresponding coil at a single frequency (mono-resonant) [44].

Received: 06/11/2025; Revised: 01/12/2025; Accepted: 04/12/2025; Published: 22/12/2025

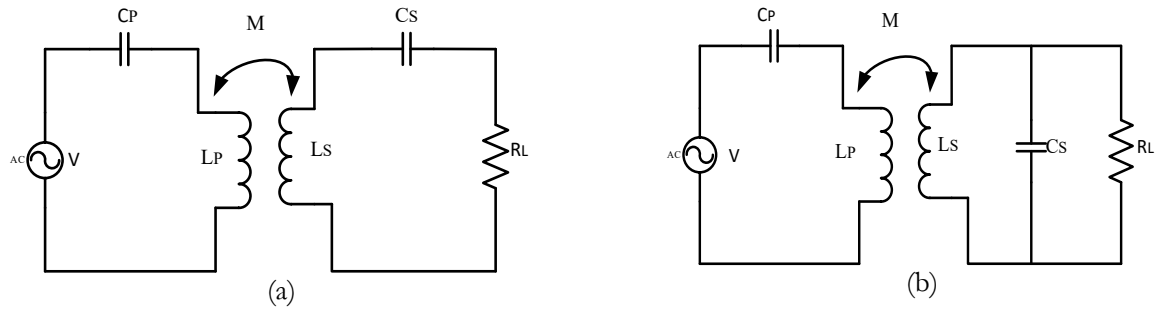

Figure 4: Equivalent circuit of series compensation (a) series–series. (b) series–parallel topology [13]

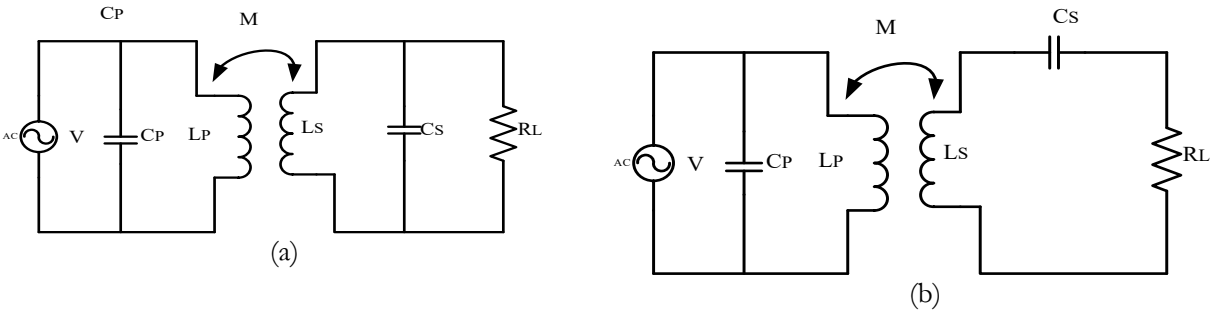

Figure 5: Equivalent circuit of parallel compensation (a) parallel–parallel topology (b) parallel–series topology [13]

1.5 Wireless Power Transfer System

Generally, circuit diagram of WPT using series-series compensation is represented in fig.6. The whole circuit has two sides, one is transmitter and the other is the receiver. DC voltage is applied to the primary as a source voltage and then H-bridge inverter is connected to generate high frequency AC voltage. Combination of capacitor and inductor which serves as compensation circuit is connected for the circuit to operate a resonance frequency[16]. For the secondary side, full bridge rectifier is connected to convert high frequency AC to DC, the DC link capacitor is connected to filter the rectified DC signals. However, a DC-DC boost converter is connected to step up the voltage to the desired value of the battery state of charge (SoC).

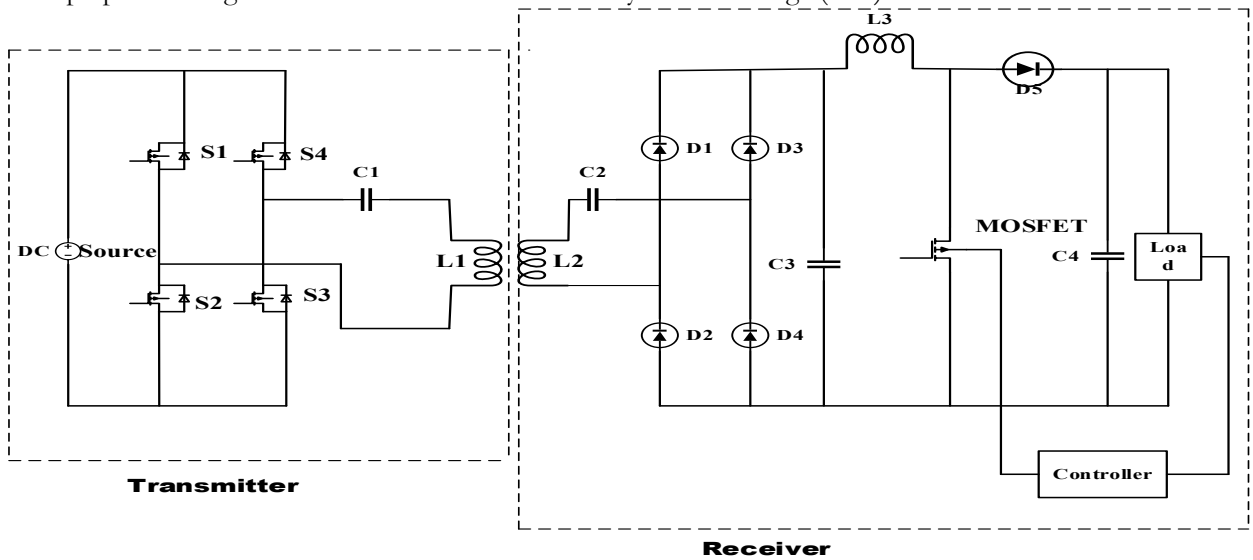

Figure 6: Circuit diagram of wireless power transfer by using SS-compensation topology

2.0 Methodology

This section described the logical framework adopted to accomplish the results of the research objectives. The process involved five major steps: literature review, system modeling, controller development, simulation and performance evaluation and comparative analysis. The materials used in this research are the Matlab/Simulink software version R2021a and the hardware is a personal computer.

Received: 06/11/2025; Revised: 01/12/2025; Accepted: 04/12/2025; Published: 22/12/2025

2.1 Mathematical Model

The mathematical model of system was adopted from the previous study. The model described the dynamic nature of the wireless power transfer system which incorporates the coupling coefficient, compensation topology, and system parameters of both primary and secondary circuits. The model served as the bedrock for the implementation and analysis of the controllers. To design a wireless power system for EV leads to find the value of different components use in the system, such as primary and secondary capacitors and inductors values, mutual induction, quality factor and coupling co-efficient. Fig. 7 shows the equivalent circuit of wireless power transfer using SS-compensation topology [7-13].

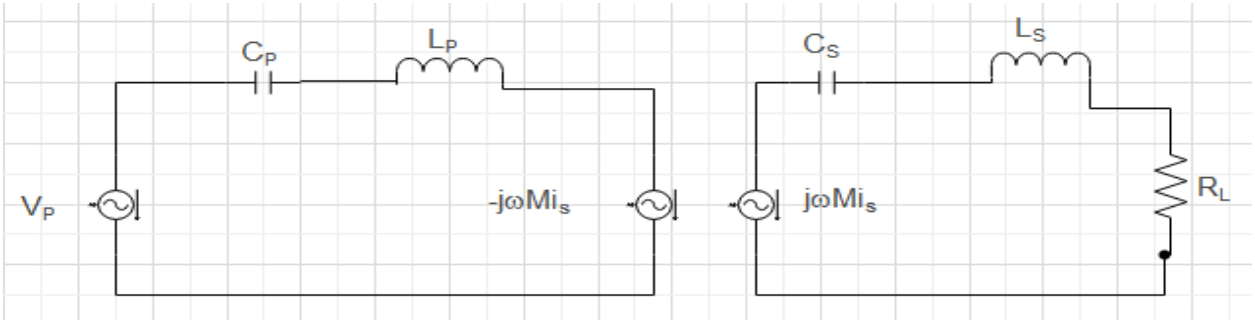

Figure 7: Equivalent circuit of WPT using SS-compensation topology [18]

By applying KVL to the primary side

$$Z_1 i_p - j\omega M i_p = V_p \quad (4)$$

where Z_1 is the primary side impedance

By applying KVL to the secondary side

$$Z_2 i_s = j\omega M i_p \quad (5)$$

where Z_2 is the secondary side impedance

Therefore, the secondary compensation capacitor can be expressed as:

$$C_S = \frac{1}{L_S \omega_O{}^2} \quad (6)$$

The primary side compensation capacitor is expressed as

$$C_P = \frac{1}{L_P \omega_o{}^2} \quad (7)$$

Secondary coil inductance can be expressed as

$$L_S = Q_S * \frac{R_L}{\omega_o} \quad (8)$$

where Q_S is the quality factor

Moreover, coefficient of coupling coil K can be expressed as

$$K = \frac{M}{\sqrt{L_P L_S}} \quad (9)$$

Primary coil inductance can be obtained from equation (9) as

$$L_P = \frac{M^2}{K^2 \times L_S} \quad (10)$$

The values of the individual component of wireless power transfer unit and their values are given in Table 1.

Table 1: Calculated parameters for transmitter and receiver coils

Parameter	**Value**	**Unit**
Transmitter self-inductance, L_P	1.437×10^{-5}	H
Receiver self-inductance, Ls	2.398×10^{-4}	H
Transmitter capacitor, C_P	2.4398×10^{-7}	F

Received: 06/11/2025; Revised: 01/12/2025; Accepted: 04/12/2025; Published: 22/12/2025

Receiver capacitor, Cs	1.462×10^{-8}	F
Mutual inductance M	1.35×10^{-5}	H
Input DC voltage, Vin	220	V
Battery voltage, V_{bat}	300-600	V
Nominal transmitter current, I_{Prms}	31.43	A
Nominal Receiver current, I_S rms	30.56	A
Operating frequency, f_O	85	kHz

2.2 Boost Converter Design

It comprises a DC input voltage source (Vs), a boost inductor (L), a controlled switch (S), a diode (D), a filter capacitor (C), and a load resistor (R). When the switch S is ON, the current through the inductor L increases linearly, while the diode D remains OFF. When S is OFF, the energy stored in L is released through D to the output R_L circuit depicted in Fig.8.

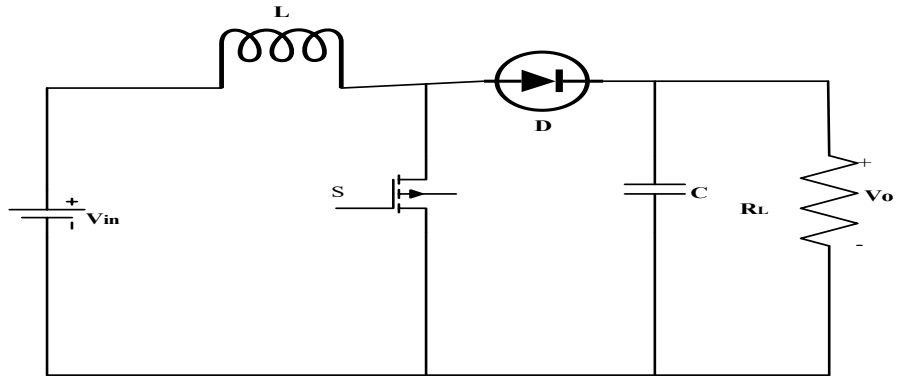

Figure 8: Boost converter circuit diagram

The design of this converter is based on the input voltage seen by the converter from the rectifier, the switching frequency was selected according to SAE standard which ranges from 20 KHz to 100 KHz. The duty cycle of the boost converter is expressed as[18].

$$D = 1 - \frac{V_{in}}{V_o} \times \eta \quad (11)$$

where V_{in} = input voltage to the converter
V_O = output voltage of the converter
η = effeciency at which the converter is expected to operate

The inductance of the converter is given by the following equation as

$$L = \frac{V_{in(max)} \times D}{f_s \times \Delta I_L} \quad (12)$$

where: L = inductance
f_S = MOSFET switching freqeuncy
ΔI_L = change in inductor current
ΔI_L = 20 to 40 % of I_L
The parameters associated with the boost converter are presented in table 2 below

Table 2: Converter components calculated values

Parameter	**Value**	**Unit**
Input voltage (V_{in})	280	V
Output voltage (V_O)	400	V
Duty cycle (D)	0.56	-
Inductance (L)	296	μH

Received: 06/11/2025; Revised: 01/12/2025; Accepted: 04/12/2025; Published: 22/12/2025

Capacitance (C)	38	μF
Load resistance (R)	32.73	Ω

2.3 Boost Converter Transfer Function

The ratio of output voltage to the duty cycle gives the transfer function (TF) of boost converter which can be expressed in Laplace form as:

$$\frac{\hat{V}_O(S)}{\hat{d}(S)} = \frac{V_O}{(1-D)^2} \times \frac{1 - S\frac{L}{R(1-D)^2}}{\left[1 + S\frac{L}{R(1-D)^2} + S^2\frac{LC}{(1-D)^2}\right]} \tag{13}$$

$$V_O = output\ voltage, D = duty\ cycle, \quad L = inductance, \quad R = resistance, \quad C = capacitance$$

By applying the calculated values of the inductor, capacitor and duty cycle from table 2 into equation (13) the transfer function of the converter can be realized as:

$$\frac{\hat{V}_O(S)}{\hat{d}(S)} = \frac{400}{(1-0.56)^2} \times \frac{1 - S\frac{2.956\times10^{-4}}{32.73(1-0.56)^2}}{\left[1 + S\frac{2.956\times10^{-4}}{32.73(1-0.56)^2} + S^2\frac{2.956\times10^{-4}\times3.80\times10^{-5}}{(1-0.56)^2}\right]} \tag{14}$$

$$\frac{\hat{V}_O(S)}{\hat{d}(S)} = TF = \frac{299.91S + 3099.17}{2.495\times10^{-3}S^2 + 0.0968S + 1} \tag{15}$$

$$TF = \frac{299.91S + 3099.17}{2.495\times10^{-3}S^2 + 0.0968S + 1} \tag{16}$$

2.4 Controller Design

The MATLAB/Simulink R2021a environment was used to create and test two advanced control strategies: Fractional Order PI (FOPI) and Fuzzy Logic Controller (FLC).

2.5 Fractional Order PI Controller

Research on fractional order control began in the early to mid-19th century with pioneers such as Liouville (1832), Holmgren (1864), and Riemann (1953). Manabe also made significant contributions in the 1960s. However, the practical use of fractional controllers was constrained by the mathematical complexity involved. With advancements in fractional calculus, the adoption of these controllers became more prevalent [19]. Fractional calculus has gained popularity recently in a number of scientific and engineering domains. The classic integral and differential operators are extended from integer order to real number order in fractional calculus. Compared to the traditional integer order one, it thus has a larger feasible scope and greater flexibility in the system modelling and controller design methodology [15]. The FOPI controller is a widely adopted solution for automatic voltage regulation (AVR) to maintain stable voltage output. Erenturk defined the general transfer function form of the FOPID controller in time domain as:

$$U(t) = K_p e(t) + K_i D^{-\lambda} e(t) + K_d D^{\mu} e(t) \tag{17}$$

In the equation above, $D^{-\lambda}$ denotes the integer of fractional order, while $D^{-\mu}$represents the fractional-order differentiator. The transfer function for the FOPID controller, derived by applying the Laplace transform to this equation, is as follows

$$\frac{U(S)}{E(S)} = K_p + \frac{K_i}{S^{\lambda}} + K_d S^{\mu} \tag{18}$$

where μ Represents the order of differentiator and the λ represents the order of integrator. The FOPI controller is a negative feedback structure as shown in fig.9. The controller was designed in Matlab using FOMCON toolbox to vary the duty cycle of the MOSFET switch of the converter. Optimal parameters were obtained by adjusting the order of fractional gain of integrator (λ), the resulting proportional, integral, and fractional gains enhanced system precision. Integral Time Square Error (ITSE) performance criterion was used to minimize the error.

Received: 06/11/2025; Revised: 01/12/2025; Accepted: 04/12/2025; Published: 22/12/2025

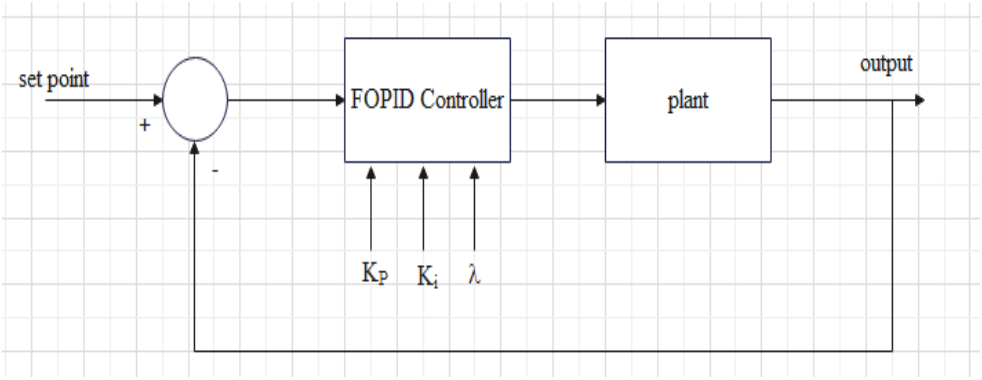

Figure 9: General block diagram of fractional PID controller [20]

2.6 Fuzzy Logic Controller

The Fuzzy Control method, which was introduced by L. A. Zadeh in 1965, performs the same tasks as the PID controller and deals with uncertainty in its mathematical model. It presents the system as a fuzzy agreement. Fuzzy logic control (FLC) is a control system where the resulting output is determined by the input state and its corresponding variation. Consequently, FLC can achieve finer voltage restoration, approaching nominal values more accurately compared to a PI controller [21]. FLC provides an inference framework that is compatible with human cognitive capacities. Fuzzy structures that make sense close to the logic. The fuzzy control system primarily consists of four components: fuzzification, rule base, fuzzy reasoning machine, and defuzzification as shown in Fig.10.

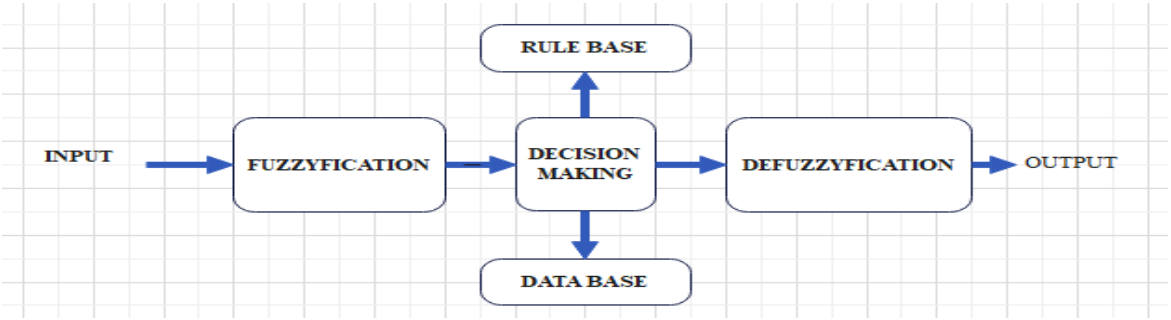

Figure 10: Fuzzy control system

Fuzzy logic controller was designed in MATLAB using FLC toolbox. Error and change in error served as inputs to the system, while converter duty cycle served as output. The membership functions and rule base were developed to handle the nature of nonlinearity of the system

2.6.1 Fuzzification

Fuzzification involves transforming input data into appropriate linguistic values, essentially converting precise facts into fuzzy sets represented by linguistic terms. The membership functions typically have triangular or trapezoidal shapes. The two most commonly used fuzzification methods are Mamdani and Sugeno [22]. The primary function is to choose the input for the fuzzy controller and convert it into a fuzzy value that the system can recognize. This involves three steps. First, the input volume is adjusted to suit the fuzzy control requirements. Second, the input is scaled. Third, the fuzzy language value for each input and the corresponding membership function are determined [23].

2.6.2 Rule Base

It comprises a fuzzy "If-Then" rule set. The fuzzy rule base includes numerous control rules and is a crucial step in translating practical control experience into fuzzy controllers [23]. The rules of the fuzzy logic algorithm are typically structured as "if and then" statements. Here, "if" specifies the condition, while "then" indicates the outcome [24]

2.6.3 Fuzzy Reasoning Machine

A variety of fuzzy reasoning machines are proposed, which primarily execute knowledge base reasoning decisions, based on either combined reasoning or independent reasoning for fuzzy rule bases.

2.6.4 Defuzzification

Received: 06/11/2025; Revised: 01/12/2025; Accepted: 04/12/2025; Published: 22/12/2025

The primary function of defuzzification is to transform the control value derived from reasoning into the control output [23].

2.6.5 Formulation of Fuzzy Rules

Fuzzy logic is a form of mathematical logic that operates on the concept of "degrees of truth," differentiating between true and false states. In designing a controller using Mamdani's fuzzy inference technique, five linguistic variables are used to quantify error (E) and change in error(dE): negatively large (NL), negatively small (NS), zero (Z), positively small (PS), and positively large (PL). Triangular and trapezoidal membership functions are employed to reduce computational complexity [24].The rule base matrix used is shown in Table 3 as:

Table 3: Fuzzy rule base matrix

Error, *E*	**Rate of change of error, de/dt**						
	NB	**NM**	**NS**	**ZE**	**PS**	**PM**	**PB**
NB	NL	NL	NM	NS	ZE	PS	PM
NM	NL	NM	NS	ZE	PS	PM	PL
NS	NM	NS	ZE	PS	PM	PL	PL
ZE	NS	ZE	PS	PM	PL	PL	PL
PS	ZE	PS	PM	PL	PL	PL	PL
PM	PS	PM	PL	PL	PL	PL	PL
PB	PM	PL	PL	PL	PL	PL	PL

where:$e = \text{error}$, $de/dt = \text{change in error}$, NB = negative big, NM = negative medium, NS = negative small, ZE = zero error, PS = positive small, PM = positive medium, and PB = positive big.

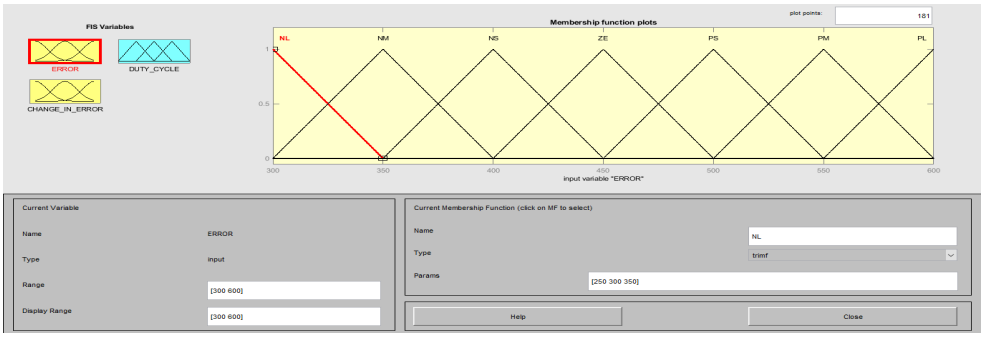

Figure 11: Input error membership function

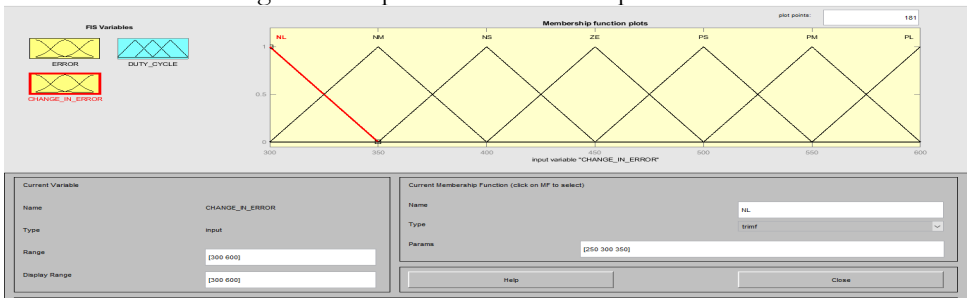

Figure 12: Input rate of change of error membership function

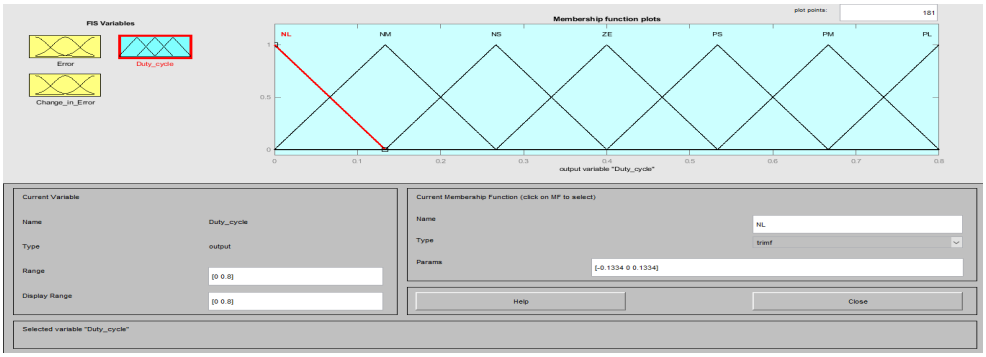

Figure 13: Output duty cycle membership function

Received: 06/11/2025; Revised: 01/12/2025; Accepted: 04/12/2025; Published: 22/12/2025

3.0 Results and Discussion

The simulation was conducted in MATLAB/Simulink to evaluate the dynamic performance of the EV wireless charging system under Fuzzy Logic and Fractional Order PI (FOPI) controllers. Both controllers were tested under identical conditions such as resonance circuit parameters, coupling coefficient and load resistance.

The wireless charging system for electric vehicles was modeled and simulated using MATLAB/Simulink. The system consists of a primary and secondary coil forming the inductive power transfer (IPT) link, a high-frequency inverter, a boost converter, and the vehicle-side battery load. Both the **FLC** and **FOPI** controllers were implemented to regulate the DC output voltage at 600 V under load resistance and coupling conditions. The simulation output results are presented in Figure 14 through 23.

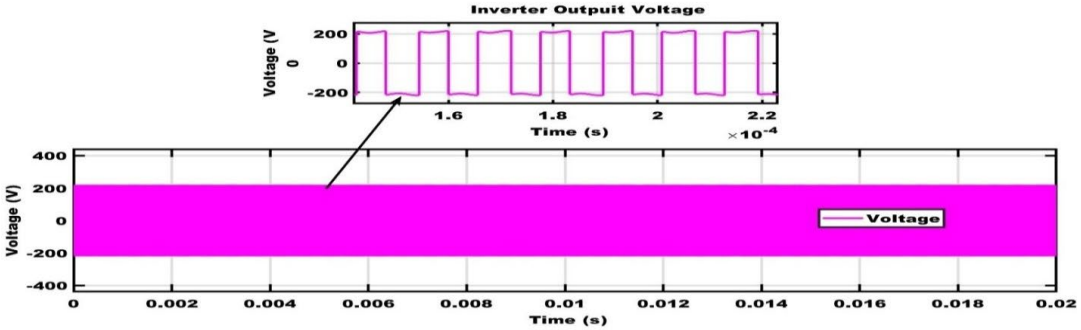

Figure 14: transmitter coil input voltage

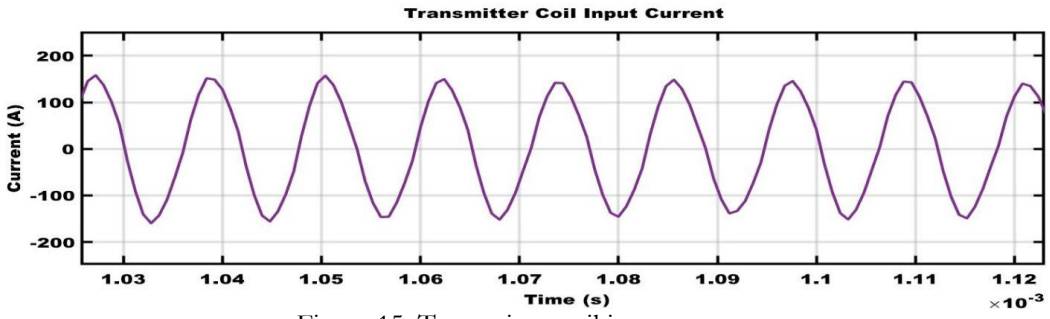

Figure 15: Transmitter coil input current

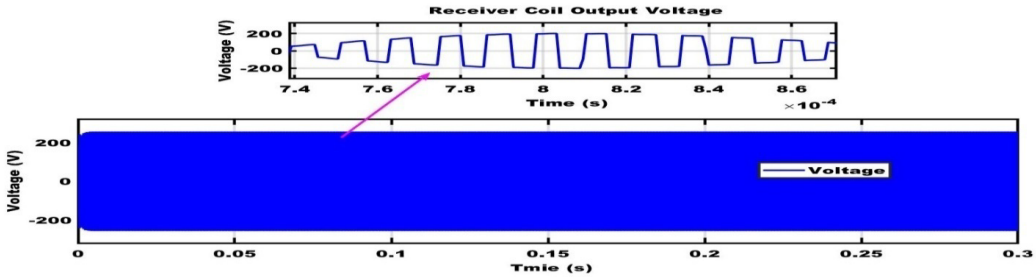

Figure 16: Receiver coil input voltage

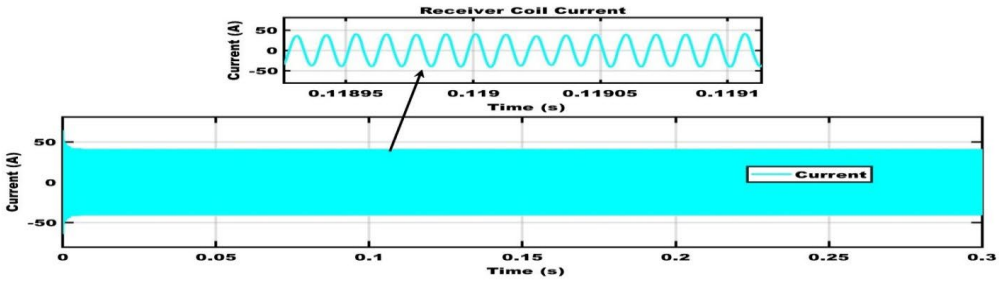

Figure 17: receiver coil input current

Received: 06/11/2025; Revised: 01/12/2025; Accepted: 04/12/2025; Published: 22/12/2025

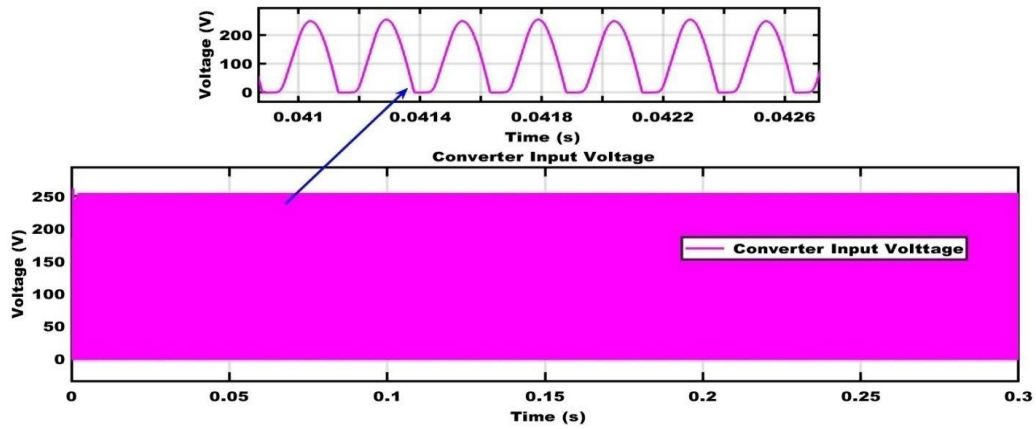

Figure 18: Converter input voltage

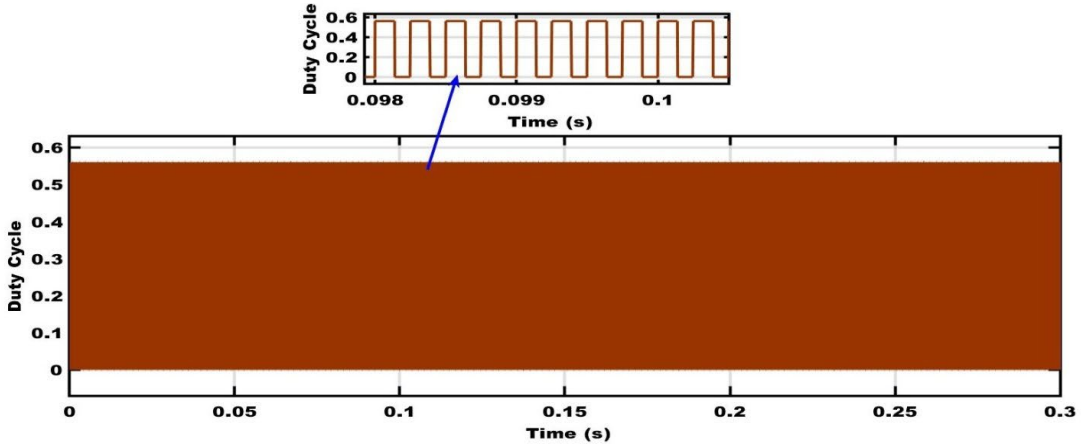

Figure 19: Converter duty cycle

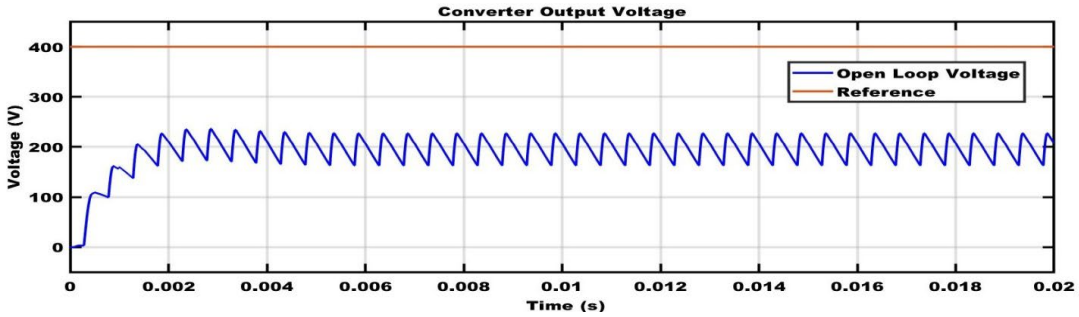

Figure 20: Converter open loop output voltage

The FOPI controller was tuned by varying the parameter λ , while the tuning of the FOPID controller was performed based on the transfer function defined in Equation (26). Through systematic adjustment of $\lambda$the FOPI controller yielded optimal parameter values. The corresponding simulation outcomes for the controller tuning are presented in Figure 21.

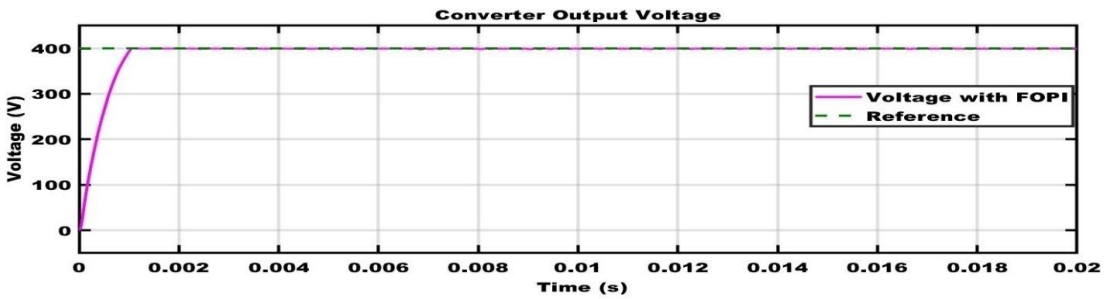

Figure 21: Output voltage with FOPI controller

Received: 06/11/2025; Revised: 01/12/2025; Accepted: 04/12/2025; Published: 22/12/2025

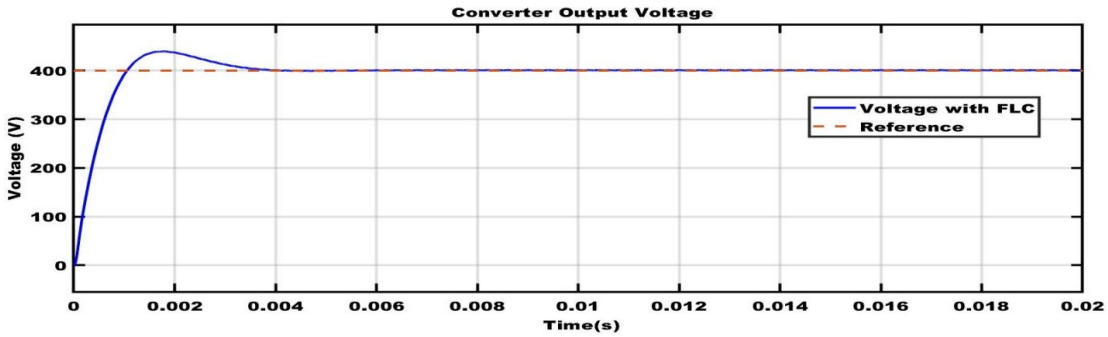

Figure 22: Output voltage with FLC controller

The simulated results of FLC and FOPI controllers are presented in Figure 25. The system with FLC has high over short compared to that of FOPI as indicated in Table 4

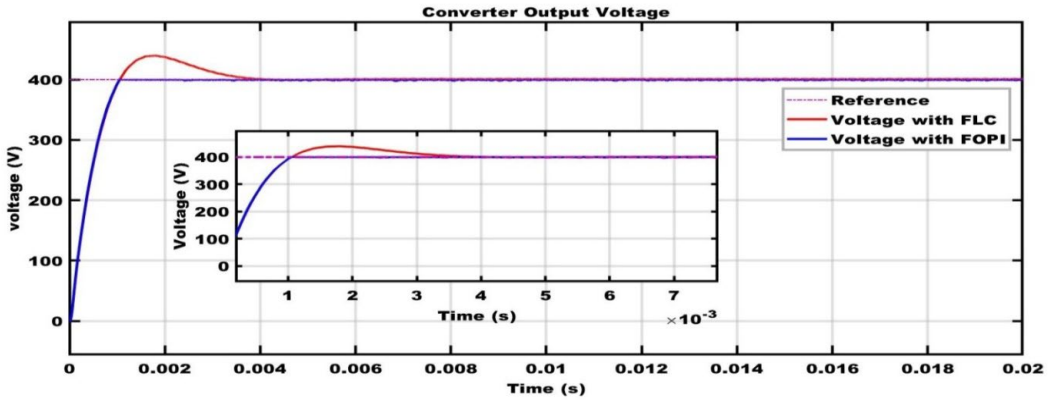

Figure 23: Output voltage response of the EV wireless charging system under FLC and FOPI controllers

Table 4: Comparative time domain analysis for open loop, FOPI and FLC

Type of system	Rise Time $(10\% - 90\%)$ (s)	Overshoot (%)	Settling Time (s)	Peak
With Fuzzy Controller	0.934	9.6302	3.9933e-03	407.8061
With FOPI Controller	0.917	0.4676	1.2373e-03	401.1227
Open Loop System	1.5944e-03	3.8945	1.5944e-03	222.7381

The power transfer efficiency of both open and close loop systems can be expressed in terms of input and output power as:

$$efficiency\ (\eta) = \frac{outputpower(P_{out})}{inputpower(P_{in})} \times 100\%$$

After running the simulation using calculated load resistance of 32.37Ω, the efficiency of the system for both open loop and close loop presented in Table 5.

Table 5: Power transfer efficiency for calculated load resistance of 32.73Ω

Type of System	Load Resistance (Ω)	Power Transfer Efficiency (η)
System With Fuzzy Controller	32.73	89%
System With FOPI Controller	32.73	72%
Open Loop System	32.73	21.8%

4.0 Conclusion and Recommendation

4.1 Conclusion

In this study, the performance of Fuzzy Logic Controllers (FLC) and Fractional Order PI (FOPI) Controllers was evaluated for an Electric Vehicle (EV) Wireless Charging System. Simulation results demonstrated that both controllers enhanced the system's stability, charging efficiency, and robustness against disturbances compared to

Received: 06/11/2025; Revised: 01/12/2025; Accepted: 04/12/2025; Published: 22/12/2025

open loop system. However, the FOPI controller outperformed the FLC in terms of minimum overshoot of 0.4676% and faster settling time$1.2373e-03s$ as indicated in table 4. While FLC is superior over FOPI controller in terms of power transfer efficiency of 89% as shown in table 5. These findings highlight the potential of Fractional Order PI and FLC controllers in terms of power transfer efficiency and time domain analysis in EV wireless charging system.

4.2 Recommendation

Based on the outcomes of this research, it is recommended that future studies explore the practical implementation of FOPI and FLC controllers in real-time wireless EV charging prototypes to validate the simulation results. The impact of environmental factors, such as temperature variation and misalignment between the transmitter and receiver coils, should be considered in future work to develop more resilient and efficient wireless charging systems.

References

[1] A. F. Nardoto, A. E. A. Amorim, L. F. Encarnação, W. M. Santos, E. J. Bueno, and D. M. Blanco, "Model predictive control for solid state transformer," *Electric Power Systems Research*, vol. 223, p. 109658, Oct. 2023, doi: 10.1016/j.epsr.2023.109658.

[2] S. Mateen, M. Amir, A. Haque, and F. I. Bakhsh, "Ultra-fast charging of electric vehicles: A review of power electronics converter, grid stability and optimal battery consideration in multi-energy systems," *Sustainable Energy, Grids and Networks*, vol. 35, p. 101112, Sep. 2023, doi: 10.1016/j.segan.2023.101112.

[3] A. Srivastava, M. Manas, and R. K. Dubey, "Electric vehicle integration's impacts on power quality in distribution network and associated mitigation measures: a review," *J. Eng. Appl. Sci.*, vol. 70, no. 1, p. 32, Dec. 2023, doi: 10.1186/s44147-023-00193-w.

[4] H. Shadfar, M. Ghorbani Pashakolaei, and A. Akbari Foroud, "Solid-state transformers: An overview of the concept, topology, and its applications in the smart grid,"*Int Trans Electr Energ Syst*, vol. 31, no. 9, Sep. 2021, doi: 10.1002/2050-7038.12996.

[5] B. Latha, M. M. Irfan, A. Flah, V. Blazek, L. Prokop, and S. S. Rangarajan, "Advances in EV wireless charging technology – A systematic review and future trends," *e-Prime - Advances in Electrical Engineering, Electronics and Energy*, vol. 10, p. 100765, Dec. 2024, doi: 10.1016/j.prime.2024.100765.

[6] M. B. Sidiku, E. M. Eronu, and E. C. Ashigwuike, "A review on wireless power transfer: Concepts, implementations, challenges, and mitigation scheme," *Nig. J. Tech.*, vol. 39, no. 4, pp. 1206–1215, Mar. 2021, doi: 10.4314/njt.v39i4.29.

[7] A. A. S. Mohamed, A. A. Shaier, H. Metwally, and S. I. Selem, "Wireless charging technologies for electric vehicles: Inductive, capacitive, and magnetic gear," *IET Power Electronics*, vol. 17, no. 16, pp. 3139–3165, Dec. 2024, doi: 10.1049/pel2.12624.

[8] V. B. Vu, "Multiphase Wireless Dynamic Charging Systems for Electric Vehicles".

[9] G. Palani, U. Sengamalai, P. Vishnuram, and B. Nastasi, "Challenges and Barriers of Wireless Charging Technologies for Electric Vehicles," *Energies*, vol. 16, no. 5, p. 2138, Feb. 2023, doi: 10.3390/en16052138.

[10] Z. Xue, W. Liu, C. Liu, and K. T. Chau, "Critical Review of Wireless Charging Technologies for Electric Vehicles," *WEVJ*, vol. 16, no. 2, p. 65, Jan. 2025, doi: 10.3390/wevj16020065.

[11] B. P. Babu, V. Karthik, M. Musharraf, A. H. Alkhayyat, and D. Dua, "Design and Development of High Frequency Inverter for Wireless Power Transfer Application," *E3S Web Conf.*, vol. 391, p. 01187, 2023, doi: 10.1051/e3sconf/202339101187.

[12] B. Latha, M. M. Irfan, B. K. Reddy, and C. H. H. Basha, "A novel enhancing electric vehicle charging: an updated analysis of wireless power transfer compensation topologies," *Discov Appl Sci*, vol. 7, no. 4, Mar. 2025, doi: 10.1007/s42452-025-06630-0.

[13] H. A. Azzawi, S. A. Gitaffa, and N. M. Ameen, "Performance and Robustness Enhancement of Fractional Order Controller (FOC) for Electric Vehicles (EV) Using Intelligent Swarms," *JESA*, vol. 56, no. 5, pp. 879–887, Oct. 2023, doi: 10.18280/jesa.560519.

[14] E. K. Ibrahim, A. H. Issa, and S. A. Gitaffa, "Optimization and Performance Analysis of Fractional Order PID Controller for DC Motor Speed Control," *JESA*, vol. 55, no. 6, pp. 723–739, Dec. 2022, doi: 10.18280/jesa.550605.

[15] M. A. George, D. V. Kamat, and C. P. Kurian, "Electric vehicle speed tracking control using an ANFIS-based fractional order PID controller," *Journal of King Saud University - Engineering Sciences*, p. S1018363922000010, Jan. 2022, doi: 10.1016/j.jksues.2022.01.001.

[16] P. R. Shabarish, R. P. Krishna, B. Prasanth, K. Deepa, P. V. Manitha, and V. Sailaja, "Fuzzy based Approach to Enhance the Wireless Charging System in Electric Vehicles," in *2020 4th International Conference on Electronics, Communication and Aerospace Technology (ICECA)*, Coimbatore, India: IEEE, Nov. 2020, pp. 176–181. doi: 10.1109/ICECA49313.2020.9297505.

Received: 06/11/2025; Revised: 01/12/2025; Accepted: 04/12/2025; Published: 22/12/2025

[17] N. Mohamed *et al.*, "A Comprehensive Analysis of Wireless Charging Systems for Electric Vehicles," *IEEE Access*, vol. 10, pp. 43865–43881, 2022, doi: 10.1109/ACCESS.2022.3168727.
[18] M. Khalilian, "Control of Wireless Power Transfer System for Dynamic Charging of Electric Vehicle".
[19] S. Sondhi and Y. V. Hote, "Fractional Order Controller and its Applications: A Review," in *Modelling, Identification and Control / 770: Advances in Computer Science and Engineering*, Phuket, Thailand: ACTAPRESS, 2012. doi: 10.2316/P.2012.769-089.
[20] P. Shah and S. Agashe, "Review of fractional PID controller," *Mechatronics*, vol. 38, pp. 29–41, Sep. 2016, doi: 10.1016/j.mechatronics.2016.06.005.
[21] R. Uthra, D. Suchitra, T. S. Babu, and B. Aljafari, "Fuzzy-Based EV Charging Station and DVR-Fed Voltage Compensation for a DFIG-Fed Wind Energy System during Grid Faults," *International Transactions on Electrical Energy Systems*, vol. 2022, pp. 1–22, Jul. 2022, doi: 10.1155/2022/1860266.
[22] C. P. Ugale, R. B. Dhumale, and V. V. Dixit, "DC-DC Converter Using Fuzzy Logic Controller," vol. 02, no. 04.
[23] J. Lin, J. Zhou, M. Lu, H. Wang, and A. Yi, "Design of Robust Adaptive Fuzzy Controller for a Class of Single-Input Single-Output (SISO) Uncertain Nonlinear Systems," *Mathematical Problems in Engineering*, vol. 2020, pp. 1–11, Mar. 2020, doi: 10.1155/2020/6178678.
[24] Z. M'barki, K. Senhaji Rhazi, and Y. Mejdoub, "A novel fuzzy logic control for a zero current switching-based buck converter to mitigate conducted electromagnetic interference," *IJECE*, vol. 13, no. 2, p. 1423, Apr. 2023, doi: 10.11591/ijece.v13i2.pp1423-1436.

Received: 06/11/2025; Revised: 01/12/2025; Accepted: 04/12/2025; Published: 22/12/2025